

# MAGNETIZATION, RUTHERFORD BACKSCATTERING SPECTROSCOPY (RBS), AND X-RAY PHOTOELECTRON SPECTROSCOPY (XPS) STUDIES OF MANGANESE-PHOSPHATE GLASSES

G. D. Khattak\*, A. S. Al-Harhi, and M. A. Salim

*Department of Physics  
King Fahd University of Petroleum and Minerals  
Dhahran, Saudi Arabia*

## الخلاصة :

تمت دراسة زجاج مكون المنجنيز والفوسفات على زجاج الفوسفات  $[(\text{MnO}_2)_x (\text{P}_2\text{O}_5)_{1-x}]$  الذي يحتوي على  $\text{MnO}_2$  بالنسب  $(x = 0.10, 0.15, 0.20, 0.30, 0.40)$  وذلك عن طريق المغنطة ومطيافية رذافور للتشتت الارتدادي (RBS)، وطيف الالكترونات الناتجة عن تعرض الزجاج للأشعة السينية (XPS). لقد لوحظ تغير تكويني عند الانتقال من المكونات الأولية إلى مكونات الزجاج، ويظهر هذا التغير واضحاً عندما يكون تركيز المنجنيز منخفضاً. لقد تم تعيين النسبة  $[\text{Mn}^{2+}/\text{Mn}_{\text{total}}]$  بدلالة  $x$  من دراسة المغنطة ونتائج RBS. ولم يمكن الاستفادة من دراسة طيف XPS لإيجاد قيم واضحة لتلك النسبة. من خلال دراسة طيف الالكترونات الناتجة عن تعرض الزجاج للأشعة السينية لوحظت خاصية مميزة لخطوط طيف  $\text{Mn } 2p$  وتتمثل في ارتفاع قيمة  $2p$  إلى طاقة ربط أعلى مقارنة ببودرة  $\text{MnO}_2$  ولعلّ تشكل معادن الفوسفات يكون السبب الرئيس لهذا الارتفاع.

\*Address for correspondence:

KFUPM Box 1854

King Fahd University of Petroleum & Minerals

Dhahran 31261

Saudi Arabia

## ABSTRACT

Phosphate glasses containing  $\text{MnO}_2$  with nominal composition  $[(\text{MnO}_2)_x (\text{P}_2\text{O}_5)_{1-x}]$ ,  $x = 0.10, 0.15, 0.20, 0.30,$  and  $0.40$  were studied by magnetization, Rutherford back-scattering spectrometry (RBS), and X-ray photoelectron spectroscopy (XPS). It is observed that compositional changes take place in going from batch to glass and that the changes are more pronounced for low Mn concentration. The ratio  $[\text{Mn}^{2+}/\text{Mn}_{\text{total}}]$  as a function of  $x$  was determined from the magnetization data combined with RBS results. However, unambiguous values of the ratio could not be determined from the XPS studies. In the XPS study of these glasses, one notable feature of the Mn  $2p$  spectra is the shift in the  $2p$  peaks to higher binding energy compared with  $\text{MnO}_2$  powder. Perhaps formation of metal phosphates could be the dominant process responsible for the high energy shift of the metal  $2p$  levels.

# MAGNETIZATION, RUTHERFORD BACKSCATTERING SPECTROSCOPY (RBS), AND X-RAY PHOTOELECTRON SPECTROSCOPY (XPS) STUDIES OF MANGANESE-PHOSPHATE GLASSES

## 1. INTRODUCTION

Transition metal ions characterized by partially filled *d*-shells can frequently exist in a number of oxidation states [1] and electronic conduction can occur as a result of electron transfer from ions in a lower oxidation state to ones in a higher oxidation state [2].

The relative proportion of transition metal ions in different oxidation states has been used in many studies as a parameter which may be related to electronic conduction [3–5]. Manganese can exist in various glasses in two oxidation states,  $Mn^{2+}$  and  $Mn^{3+}$  [3]. Each of these has a different electronic structure and coordination geometry. Thus, the structures and properties of such glasses (electrical, optical, magnetic, mechanical, *etc.*) depend on the relative proportion of different valence states of manganese. Hence to understand the effect of manganese valence states on the structure and properties of these glasses, it is important to control and measure the ratio of  $Mn^{2+}$  and  $Mn^{3+}$ . The ground state of  $Mn^{2+}$  is  ${}^6S_{5/2}$  ( $J = S = 5/2$ ) and that of  $Mn^{3+}$  is  ${}^5D_0$  ( $J = 0, S = 2$ ) and thus both exhibit paramagnetism. In general, electron spin resonance (ESR) spectroscopy technique is used for the study of paramagnetic centers in glass systems [6, 7]. In the present work we attempted to use magnetization and X-ray photoelectron spectroscopy (XPS) studies to find the ratio of  $Mn^{2+}$  and  $Mn^{3+}$  in these manganese phosphate glasses.

Furthermore, when phosphate glasses are prepared, phosphates which are not connected with a cation react with moisture in the air and produce phosphoric acid during melting which easily vaporizes at higher temperature [8]. Thus the composition of the glass may be different from that of the batch and may also influence the relative proportion of the different valence states in the glass. Hence, in the present work the relative atomic concentrations of Mn, P, and O were determined using Rutherford backscattering spectrometry (RBS). Thus RBS will give the number of Mn ions/gram of the sample and this number can be used to find the ratio of  $Mn^{2+}$  and  $Mn^{3+}$  from the magnetization data. Initially the idea was to compare this ratio with that obtained from XPS; however, it was found that unambiguous values of the ratio could not be determined from the XPS results.

## 2. EXPERIMENTAL PROCEDURE

The glasses were prepared by melting dry mixtures of  $MnO_2$  and  $P_2O_5$ , in alumina crucibles, with the composition  $[(MnO_2)_x(P_2O_5)_{1-x}]$ , where  $x = 0.10, 0.15, 0.20, 0.30,$  and  $0.40$ . All chemicals used in this study were of reagent grade. The oxidation and reduction reactions in a glass melt are known to depend on the size of the melt, the sample geometry, whether the melt is static or stirred, thermal history, and quenching rate. To keep these factors constant, all glass samples were prepared under the same conditions. About 40 g of chemicals were mixed to obtain homogenized batches. The crucible containing the batch was placed in a furnace and heated at  $300^\circ C$  for an hour prior to melting the mixture in order to minimize volatilization. The crucible was then transferred to a melting furnace maintained at a temperature of  $1330^\circ C$ . The melt was left for about 4 hours under atmospheric conditions in the furnace. During this time the melt was occasionally stirred with an alumina rod. The homogenized melt was then cast onto a stainless steel plate mold. The samples were disk shaped with a diameter of  $\sim 1.5$  cm and thickness of about 3 mm. This procedure gave samples with satisfactory glassy appearance without detectable presence of air bubbles or apparent devitrification. The absence of crystallites was checked visually and by X-ray analysis.

The RBS was performed with 2 MeV  $He^{2+}$ , as described elsewhere [9]. Briefly, a solid state detector (Tennelec model PD-50-100-14-CB) was placed in the chamber at a scattering angle of  $164^\circ$ , with an effective solid angle of 1.75 msr. The composition of each sample was measured with an accuracy greater than  $\pm 3\%$  for a large beam spot (diameter  $> 2$  mm) and each sample was measured at least twice. A gold film deposited on a silicon substrate was used in calibrating the channel-energy scale of the detection system. The collected RBS spectra were then fitted by the code RUMP [10] to find the relative concentrations of various elements in the sample. A compositional uncertainty of about 5% results from the code RUMP fits which takes into account uncertainties in the differential scattering cross-sections between projectile and target atoms, stopping cross-sections and statistical fluctuations.

The field-dependent DC magnetization measurements were performed by an EG&G Princeton Applied Research (PAR) Model 155 vibrating sample magnetometer (VSM) at room temperature with applied fields ranging from 0 to 10 kOe. The temperature-dependent measurements were also performed on the VSM using a 1 kOe field strength, with the temperature being slowly swept from 7 K to room temperature. The data have been corrected for the sample holder magnetization, which was measured after each sample measurement. The overall accuracy of the magnetization measurements is estimated to be approximately  $\pm 5\%$ .

The XPS measurements were carried out with a V.G. Scientific ESCALAB MKII spectrometer equipped with dual aluminum–magnesium anodes. Details of the system are given elsewhere [11]. The energy scale of the spectrometer was calibrated using Cu  $2p_{3/2} = 932.4$  eV and the energy separation between Cu  $2p_{3/2}$  and Cu  $2p_{1/2}$  of 19.8 eV. The charging of non-conducting glass samples was avoided by flooding the sample with a separate source of low-energy electrons. The energy and intensity of these external electrons were adjusted to obtain the best resolution as judged by the narrowing of the full width at half maximum (FWHM) of the photoelectron peaks. It was found that at the optimum settings of the neutralizing gun (electron kinetic energy between 5 to 10 eV and electron emission current at the sample between 1 and 5 nA), the position of the adventitious C 1s line was within  $\pm 0.5$  eV of 284.6 eV. This peak arises due to hydrocarbon contamination and its binding energy is generally accepted as remaining constant irrespective of the chemical state of the sample. For the sake of consistency all energies are reported with reference to the C 1s transition at 284.6 eV. For XPS measurements, standard oxide powder samples were embedded in substrates of indium foil supported by metallic backing. The samples were loaded through a fast entry airlock into a preparation chamber and finally into the analysis vessel. The base pressure in the analysis chamber during these measurements was less than  $5 \times 10^{-11}$  mbar.

### 3. RESULTS AND DISCUSSION

A typical RBS spectrum for a glass sample is shown in Figure 1. Edges of the overlapping bands corresponding to the elements Mn, P, and O are seen. The collected RBS spectra (dots) were then fitted (continuous curve) by the code RUMP [10] to find the relative concentrations of various elements in the glass. Spectra similar to this were obtained for the other compositions. The results are given in Table 1.

The results of the magnetization  $M$  as a function of the magnetic field  $H$  at room temperature are shown in Figure 2 as plots of  $M$  vs  $H/T$ . In a magnetic field, an atom with angular momentum quantum number  $J$  has  $2J+1$  equally spaced energy levels. The magnetization  $M$  is then given by

$$M = NgJ\mu_B B_J(x) \text{ with } x \equiv \frac{gJ\mu_B H}{k_B T}, \quad (1)$$

**Table 1. Phosphorus-to-Manganese Atomic Ratio  $R = P/Mn$  and Oxygen-to-Phosphorus Atomic Ratio  $R^* = O/P$  for Manganese–Phosphate Glasses.**

Metal	$x$ (nominal)	$R(P/Mn)$ Batch (nominal)	$R(P/Mn)$ Glass (RBS)	$R^*(O/P)$ Batch (nominal)	$R^*(O/P)$ Glass (RBS)
Mn	0.10	18.00	2.91	2.61	2.75
	0.15	11.33	2.81	2.67	2.69
	0.20	8.00	2.78	2.75	2.64
	0.30	4.66	2.83	2.93	2.90
	0.40	3.00	2.21	3.17	3.07

where  $\mu_B$  is Bohr magnetron,  $k_B$  the Boltzmann constant,  $g = 2$ ,  $J = 5/2$  for  $Mn^{2+}$  and  $J = 2$  for  $Mn^{3+}$ , and  $B_J(x)$  is the Brillouin function defined as

$$B_J(x) = [(2J + 1)/2J] \coth[(2J + 1)x/2J] - \left[ \left( \frac{1}{2J} \right) \coth\left( \frac{x}{2J} \right) \right],$$

realizing that even at room temperature, Equation (1) reduces to the usual functional form of

$$M = N J(J+1)g^2 \mu_B^2 H/3k_B T. \tag{2}$$

The magnetization data for the glasses were fitted to Equation (2) with two terms: a contribution from the  $Mn^{2+}$  ions ( $J = 5/2$ ) and the contribution from  $Mn^{3+}$  ions ( $S = 2$ ) as follows:

$$\begin{aligned} M_{total} (\text{emu/gram}) &= M(Mn^{2+}) + M(Mn^{3+}) \\ &= N_1 J(J+1)g^2 \mu_B^2 H/3k_B T|_{J=5/2} + (N - N_1) J(J+1)g^2 \mu_B^2/3k_B T|_{J=2} \end{aligned}$$

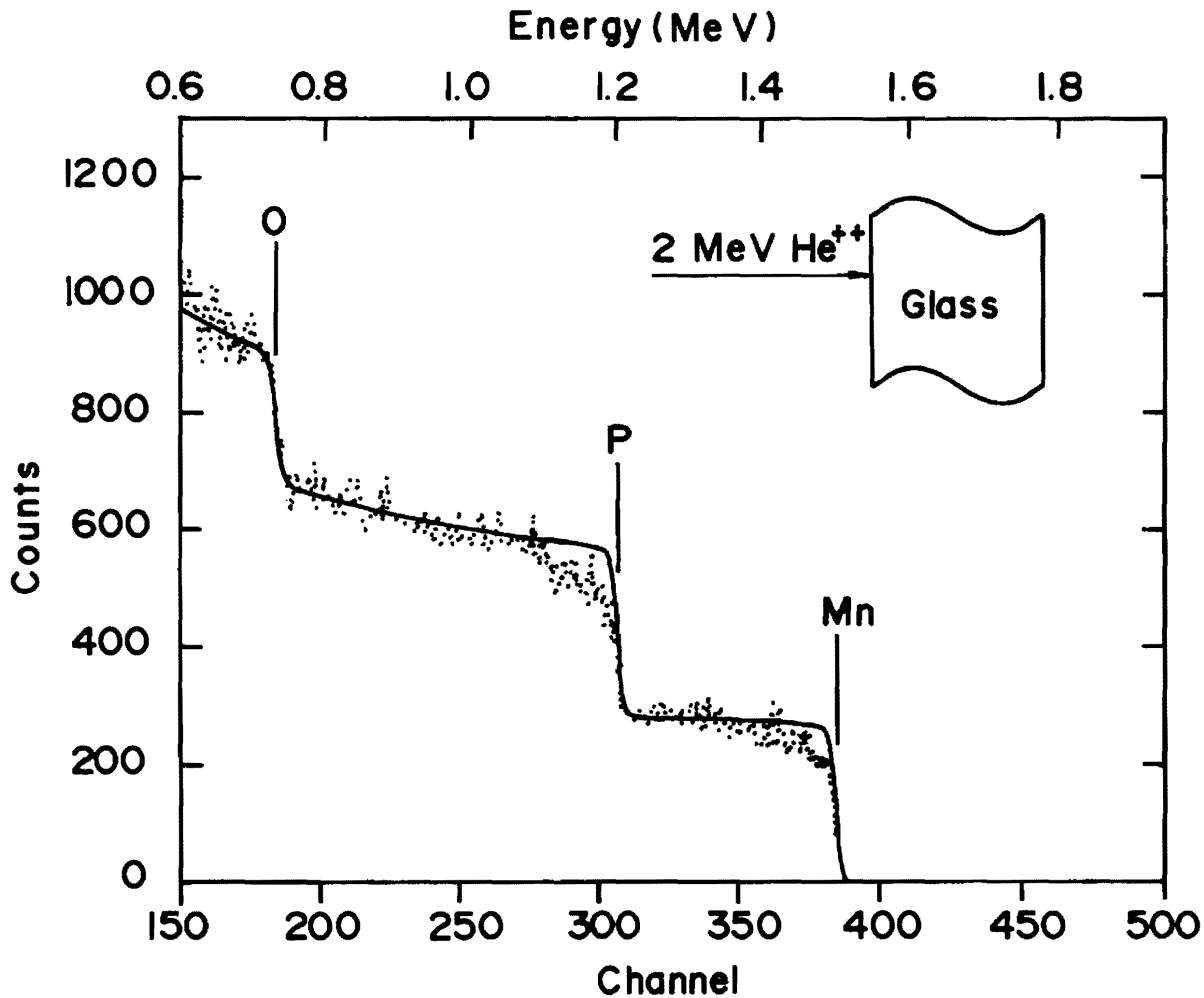


Figure 1. RBS Spectrum ( $2 \text{ MeV } ^4\text{He}^{2+}$  Analysis) of a Glass Sample with Composition  $[(MnO_2)_{0.15}(P_2O_5)_{0.85}]$  (.....) Overlaid with the Corresponding Fit (—) as Generated by the Code RUMP (Reference [10]).

where  $N$  is the total number of Mn ions/gram of the sample obtained from the RBS data. The number  $N_1$  (number of  $\text{Mn}^{2+}$  ions per gram of the sample) was used as an adjustable parameter to obtain the best fit to the experimental data. Excellent agreement was obtained which is shown by the solid lines in Figure 2. The number of  $\text{Mn}^{2+}$  ions/gram and  $\text{Mn}^{3+}$  ions/gram for each sample obtained from the fits is given in Table 2. The DC magnetic susceptibility data are also shown for a representative sample ( $x = 0.15$ ) in Figure 3 as a plot of  $1/\chi$  vs  $T$ . The susceptibility follows a Curie-Weiss behavior:  $\chi = C/(T-\theta)$ . For the temperature range of  $\approx 10$  to 300K (the highest temperature of measurements), the susceptibility results in a Curie constant of  $\approx 1.56 \times 10^{-2}$  emu K/gram and a paramagnetic Curie temperature of  $\approx -13$ K. Similar fitting of Equation (2) was also applied to the other  $1/\chi$  vs  $T$  data. The error associated with the  $M$  vs  $H/T$  data is less than 5%, while  $1/\chi$  vs  $T$  data has an uncertainty with increasing temperature. The ratio  $[\text{Mn}^{2+}/\text{Mn}_{\text{total}}]$  as a function of  $x$  is also tabulated in Table 2 and it is observed that this ratio decreases with  $x$ .

The magnetization results for these glasses cannot be explained on the basis of batch compositions. Instead, a larger concentration of Mn ions is needed to fit the data as shown in Table 2. This is in agreement with the RBS results which indicated compositional changes occurring from the batch to the glass melt. It is also clear from Table 2, that the difference between the batch composition and glass composition is larger for lower Mn concentrations in the starting material. This can be understood in terms of the  $\text{P}_2\text{O}_5$  which contains non-bridging oxygens. Thus the addition of transition metal oxides tends to strengthen the structure since the cations can locate between non-bridging oxygens.

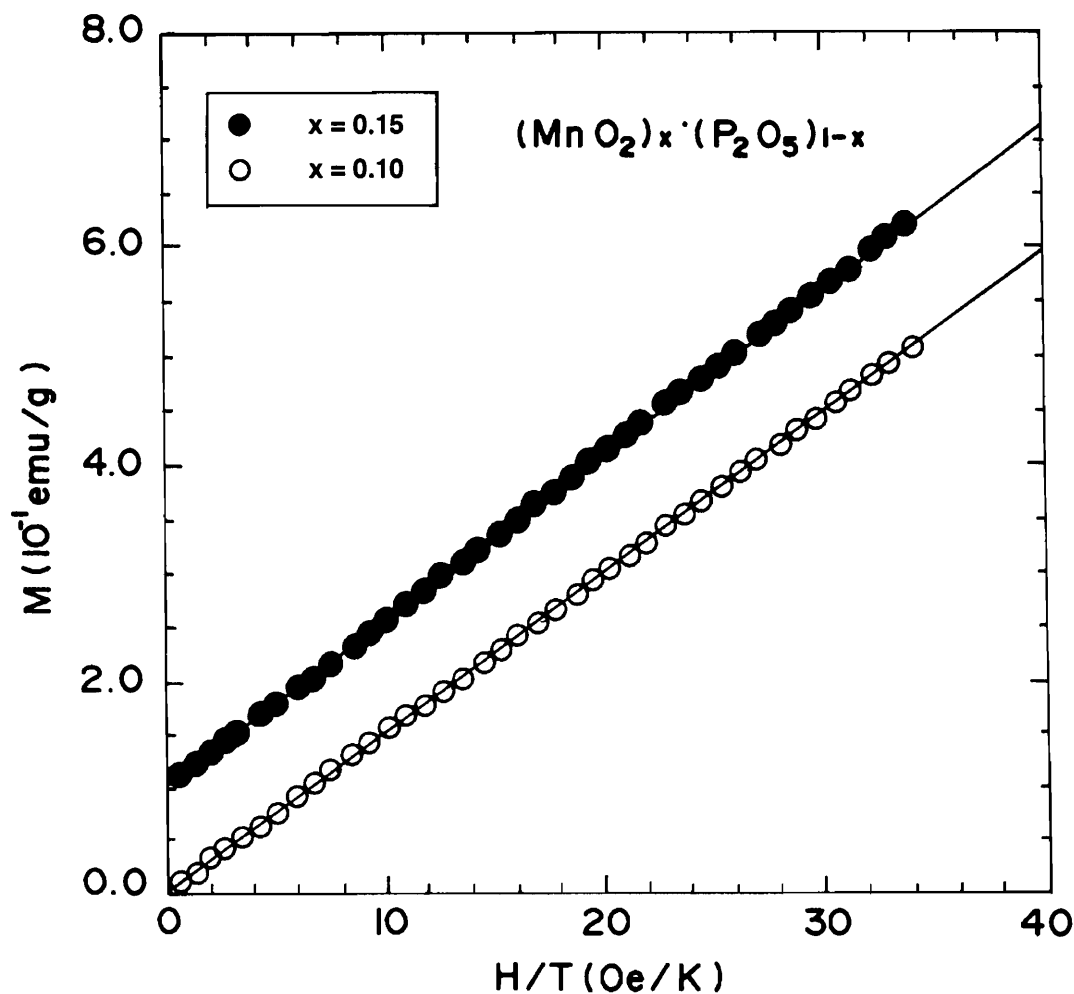


Figure 2. The Field-Dependent Magnetization  $M$  for  $[(\text{MnO}_2)_x (\text{P}_2\text{O}_5)_{1-x}]$  with  $x = 0.10$  and  $0.15$  at Room Temperature as Plots of  $M$  vs  $H/T$ . The experimental data are shown by points and the solid lines represent the fit to the data. The data for different compositions are displaced from the origin for clarity.

Phosphates which are not connected with cations react with moisture in the air to produce phosphoric acid during melting. This acid is easily fumed at high temperatures. For lower concentrations more phosphates are free to make phosphoric acid resulting in a greater loss of phosphorus and hence a larger Mn concentration in glass.

**Table 2. Mn<sub>total</sub> Ions/Gram in Batch as well as in Glass. Mn<sup>2+</sup> and Mn<sup>3+</sup> ions/gram from magnetization data and [Mn<sup>2+</sup>/Mn<sub>total</sub>] ratio (%) from magnetization and RBS for compositions [(MnO<sub>2</sub>)<sub>x</sub> - (P<sub>2</sub>O<sub>5</sub>)<sub>1-x</sub>].**

<i>x</i>	Mn <sub>total</sub> /gram (N <sub>A</sub> ) (Batch Composition)	Mn <sub>total</sub> /gram (N <sub>A</sub> ) from RBS	Mn <sup>2+</sup> /gram (N <sub>A</sub> ) from Magnetization	Mn <sup>3+</sup> /gram (N <sub>A</sub> ) from Magnetization	[Mn <sup>2+</sup> /Mn <sub>total</sub> ] (%) from Magneti- zation & RBS
0.10	0.00073	0.00366	0.00311	0.00056	85
0.15	0.00112	0.00382	0.00302	0.00079	79
0.20	0.00153	0.00388	0.00293	0.00095	76
0.30	0.00239	0.00431	0.00241	0.00189	56
0.40	0.00334	0.00366	0.00247	0.00119	67

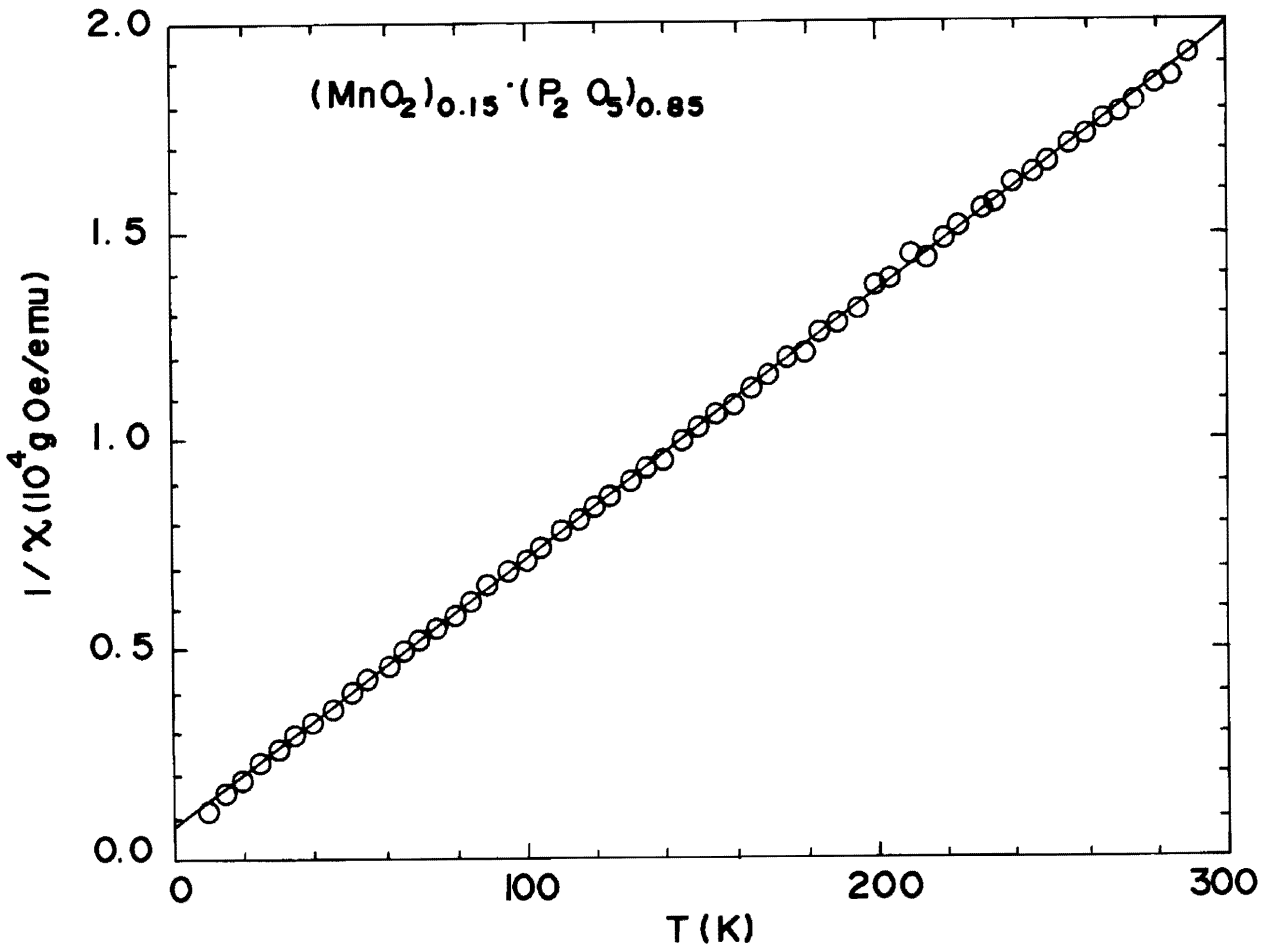


Figure 3. DC Susceptibility of [(MnO<sub>2</sub>)<sub>x</sub> (P<sub>2</sub>O<sub>5</sub>)<sub>1-x</sub>] for x = 0.15 as a Plot of 1/χ vs T. The solid line represents the Curie-Weiss behavior.

An alternative qualitative explanation for the loss of phosphorus can be given by Raoult's Law which states that the vapor pressure of the individual components in a mixture is proportional to its mole fraction. For lower Mn concentrations, the vapor pressure of the phosphate will be higher, and larger evaporation rates of the phosphorus can be expected. Thus, for a fixed melting temperature of 1330°C and time of 4 h, the largest phosphorus loss will be for the smallest Mn concentration glasses, in agreement with the experimental results.

A wide scan X-ray photoelectron spectrum for the sample with  $x = 0.40$  is shown in Figure 4. Similar spectra were obtained for the other glass compositions. These spectra were obtained using non-monochromatized Al  $K_{\alpha}$  radiation for about 1 h. Apart from the photoelectrons and Auger transitions of the glass constituents, the C 1s transition is observed. This feature at a binding energy of 284.6 eV is the usual peak associated with hydrocarbon contamination, and is almost always present on the samples introduced from the laboratory environment or from a glove box [12]. In addition, impurity atoms of Al have been detected by the observation of peaks corresponding to core levels of Al 2p at 75.6 eV and of Al 2s at 121.1 eV. These peaks are not visible in Figure 4; however, they can be seen upon magnification of the spectrum. A possible source of Al contamination could be the alumina crucibles in which the melts were formed. Crucible contamination was found to diminish as the Mn-oxide batch content was increased. However, the estimated Al concentration from the XPS results was found to be less than 2.5 atom % in all samples. Figure 5 shows the Mn 2p spectra obtained from the glass samples as well as from the MnO<sub>2</sub> powder. In the glasses one notable feature of the Mn 2p spectra, besides the appearance of a very weak contribution from a shake-up satellite (marked sat in Figure 5), is the shift in the 2p peaks to higher binding energy compared with MnO<sub>2</sub> powder. It is known [13] that the presence of non-equivalent atoms of the same element in a solid gives rise to core-level peaks with measurably different binding energies. Non-equivalence of atoms can be a result of: (a) a difference in formal oxidation state, (b) a difference in molecular environment. The binding energy increases with an increase in the oxidation state of a metal atom. In the situation where the formal oxidation state is the same, the general rule is that the core-level binding energy of the metal atom increases as the electronegativity (electron withdrawing power) of the attached atoms or

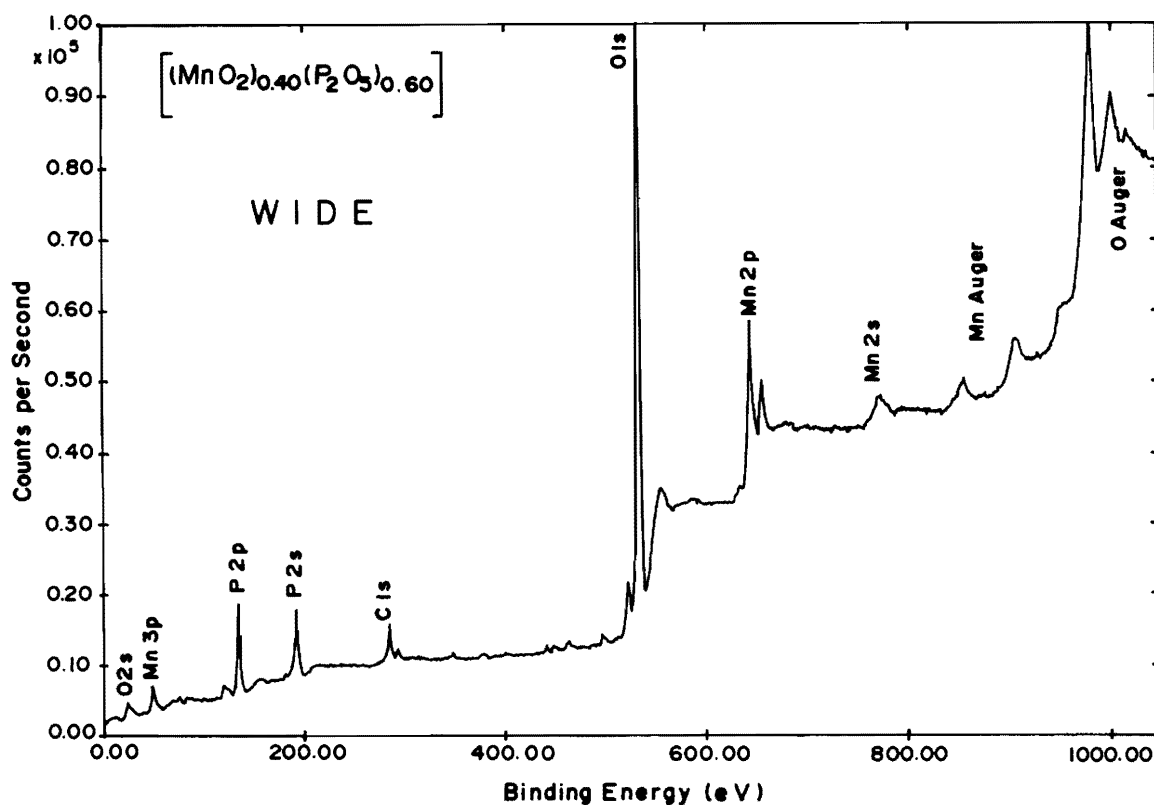


Figure 4. A Wide Scan XPS Spectra of  $(\text{MnO}_2)_x(\text{P}_2\text{O}_5)_{1-x}$  Glass with  $x = 0.40$ . Spectra given were obtained using Al  $K_{\alpha}$  ( $h\nu = 1486.6$  eV).

groups increases [13]. Trivalent ( $\text{Mn}^{3+}$ ) and divalent ( $\text{Mn}^{2+}$ ) are the two main oxidation states in which Mn exists in various glasses [1, 14]. Assuming this holds for the present samples, then Mn is reduced to the lower valence state, while going from the metal oxide powder ( $\text{Mn}^{4+}$ ) to the glass ( $\text{Mn}^{3+}$  and/or  $\text{Mn}^{2+}$ ).

It follows from the above that the process (a) cannot account for the high-energy shift of the  $2p$  level (Figure 5) upon going from metal oxide to the glass. Perhaps formation of metal phosphates (process b) could be the dominant process responsible for the high energy shift of the metal  $2p$  levels, since phosphate ions are more electronegative than oxygen [15]. In an earlier study of transition metal (Fe, Co, Ni, Cu, and Zn) in phosphate glasses, similar high-energy shifts have been observed [16].

As mentioned earlier, trivalent ( $\text{Mn}^{3+}$ ) and divalent ( $\text{Mn}^{2+}$ ) are the two main oxidation states in which Mn exists in various glasses [1, 14]. In general, to find the relative proportion of transition metal ions in different oxidation states

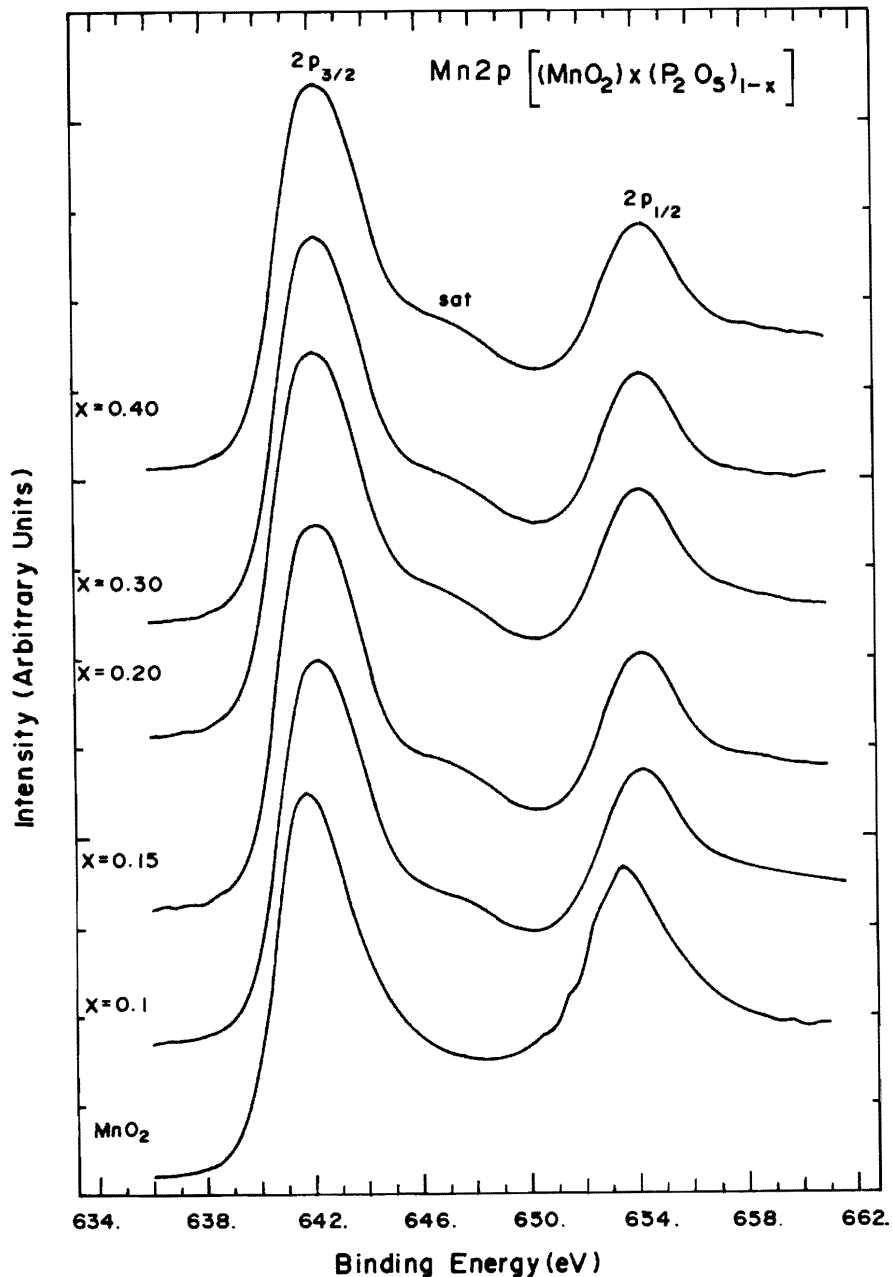


Figure 5. Core Level Spectra of the Mn 2p in  $\text{MnO}_2$  Powder and Mn-Phosphate Glasses.

from XPS studies, a deconvolution method is undertaken in which the  $2p$  spectrum is assumed to be composed of two overlapping peaks. Each component peak in the spectrum is fitted to a sum of weighted Lorentzian–Gaussian peaks with a linear sloping background by means of a least-squares fitting program [17]. Using these peak areas, the relative proportion is then determined. However for similar ligands, the high-energy shift in the  $2p$  peak while going from  $Mn^{2+}$  to  $Mn^{3+}$  may not be large enough to be resolved by XPS. For example, the Mn  $2p$  binding energies for  $Mn^{2+}$  (MnO) and  $Mn^{3+}$  ( $Mn_2O_3$ ) are observed to be at 641.7 eV and 641.8 eV respectively [17]. Similarly for the fluorides the Mn  $2p$  binding energies of  $Mn^{2+}$  ( $MnF_2$ ) and  $Mn^{3+}$  ( $MnF_3$ ) are each 642.8 eV [17]. Hence, unambiguous values of the ratio could not be determined from the present XPS studies.

#### 4. CONCLUSION

In conclusion, the results presented above have shown that compositional changes take place in going from batch to glass. These changes are dependent on  $x$  (the concentration of Mn), being largest for low  $x$  values. The ratio  $[Mn^{2+}/Mn_{total}]$  obtained from magnetic measurements is also dependent on  $x$ , and initially decreases with increasing  $x$ . However, unambiguous values of this ratio could not be determined from the XPS studies for comparison.

#### 5. ACKNOWLEDGEMENT

Support of the KFUPM Physics Department and Research Committee (Grant PH/PHYSPROP/43) is acknowledged. The assistance of Mr. M. A. Khan for experimental work is appreciated.

#### REFERENCES

- [1] C. R. Bamford, *Colour Generation and Control in Glasses*. Amsterdam: Elsevier, Scientific Publishing Company, 1977.
- [2] N. F. Mott, "Conduction in Glasses Containing Transition Metal Ions", *J. Non. Cryst. Solids*, **1** (1968), pp. 1–17.
- [3] M. Sayer and A. Mansingh, "Transport Properties of Semiconducting Phosphate Glasses", *Phys. Rev.*, **B6** (1972), pp. 4629–4643.
- [4] G. S. Linsley, A. E. Owen, and F. M. Hyayatee, "Electronic Conduction in Vanadium Phosphate Glasses", *J. Non. Cryst. Solids*, **4** (1970), pp. 208–219.
- [5] G. W. Anderson and F. U. Luehrs, "Structural Characterization of and Phase Separation in Vanadate Glasses", *J. Appl. Phys.*, **39** (1968), pp. 1634–1638.
- [6] F. R. Landsberger and P. J. Bray, "Magnetic Resonance Study of the  $V_2O_5 - P_2O_5$  Semiconducting Glass System", *Chem. Phys.*, **53** (1970), pp. 2757–2768.
- [7] C. Ananthamohan, C. A. Hogarth, and K. A. K. Lott, "An Electron Spin Resonance Study of Copper Phosphate Glasses Containing Some Rare-Earth Oxides", *J. Mater. Sci.*, **24** (1989), pp. 4423–4426.
- [8] B. S. Bae and M. C. Weinberg, "Oxidation-Reduction Equilibrium in Copper Phosphate Glass Melted in Air", *J. Am. Ceram. Soc.*, **74** (1991), pp. 3039–3045.
- [9] E. E. Khawaja, F. F. Al-Adel, A. B. Hallak, M. M. Al-Kofali, and M. A. Salim, "Rutherford Backscattering Spectroscopy and X-Ray Photoelectron Spectroscopy of Thin Glass Films Prepared by Laser Evaporation", *Thin Solid Films*, **192** (1990), pp. 149–156.
- [10] L. R. Doolittle, "A Semiautomatic Algorithm for Rutherford Backscattering Analysis", *Nucl. Instrum. Methods*, **B15** (1986), pp. 227–231.
- [11] E. E. Khawaja, Z. Hussain, M. S. Jassar, and O. B. Dabbousi, "X-Ray Photoelectron Spectroscopy Study of Vanadium Germanate Glass", *J. Non. Cryst. Solids*, **93** (1987), pp. 45–52.
- [12] G. E. Mullenberg, ed., *Handbook of X-Ray Photoelectron Spectroscopy*. Minnesota: Perkin–Elmer, Physical Electron Division, 1970.
- [13] D. Briggs and J. C. Riviere, in *Practical Surface Analysis by Auger and X-Ray Photoelectron Spectroscopy*. ed. D. Briggs and M. P. Seah. Chichester: John Wiley & Sons, 1988, p. 477.
- [14] J. Wong and C. A. Angell, *Glass Structure by Spectroscopy*. New York: Marcel Dekker, Inc., 1976.
- [15] J. E. Huheey, "The Electronegativity of Multiple Bonded Groups", *J. Phys. Chem.*, **70** (1966), pp. 2086–2092.
- [16] E. E. Khawaja, S. M. A. Durrani, F. F. Al-Adel, M. A. Salim, and M. Sakhawat Hussain, "X-Ray Photoelectron Spectroscopy and Fourier Transform Infrared Studies of Transition Metal Phosphate Glasses", *J. Mat. Sci.*, **30** (1995), pp. 2225–2234.
- [17] J. C. Carver, G. K. Schweitzer, and T. A. Carlson, "Use of X-Ray Photoelectron Spectroscopy to Study Bonding in Cr, Mn, Fe, and Co Compounds", *J. Chem. Phys.*, **57** (1972), pp. 973–982.

Paper Received 8 October 1995; Revised 25 December 1995; Accepted 8 January 1996.